

LIBRARY
Michigan State
University

This is to certify that the

thesis entitled

IMPROVED UTILITY OF MICROWAVE ENERGY
FOR SEMICONDUCTOR PLASMA PROCESSING
THROUGH RF SYSTEM STABILITY ANALYSIS AND ENHANCEMENT

presented by

Paul Rummel

has been accepted towards fulfillment
of the requirements for

Master's degree in Electrical Eng


Major professor

Date 5/8/00

PLACE IN RETURN BOX to remove this checkout from your record.
TO AVOID FINES return on or before date due.
MAY BE RECALLED with earlier due date if requested.

DATE DUE	DATE DUE	DATE DUE
		JUL 27 2004 07 27 04

**Improved Utility of Microwave Energy for Semiconductor Plasma Processing
through RF System Stability Analysis and Enhancement**

By

Paul Rummel

A THESIS

**Submitted to
Michigan State University
In partial fulfillment of the requirements
For the degree of**

MASTER OF SCIENCE

Department of Electrical and Computer Engineering

2000

ABSTRACT

Improved Utility of Microwave Energy for Semiconductor Plasma Processing through RF System Stability Analysis and Enhancement

By

Paul Rummel

The bulk of today's semiconductor plasma processing equipment utilizes RF energies at frequencies from 50 KHz to 60 MHz for deposition, etching, cleaning and various other processes. One of the impediments to utilizing microwave energy for these processes is the inherent instability often encountered with systems operating at frequencies of .5 to 2.45 GHz. Systems with plasma loads excited by resonant antennas, impedance matched by resonant circuits or cavities, and powered by generators of various source impedances are invariably unstable over some operating conditions. For microwave systems, this instability typically manifests itself as a propensity for the plasma to extinguish or rapidly change to a lower density as the impedance matching device is adjusted to minimize reflected power to the microwave generator.

This paper shows why this instability exists and how a microwave driven plasma system can be modified to achieve better stabilization. A Matlab Simulink model and a state-model control analysis are used to identify system parameters that affect system stability and to predict the results of modifying those parameters towards the goal of improving stability.

A plasma system utilizing an MPDR13 Plasma Disk Reactor is used to first characterize the developed models, and then modified to illustrate the models' predictions. A high correlation between predicted and measured system stability validates the method of using a control analysis to model plasma system stability.

TABLE OF CONTENTS

TABLE OF FIGURES.....	v
INTRODUCTION.....	1
Motivations.....	2
Goals.....	3
CHAPTER 1	
STABILITY ANALYSIS.....	5
Definition of stability.....	5
Stability quantified.....	6
Background.....	7
Definition of Variables.....	10
Plasma Impedance Curve.....	12
Delivered Power Surface.....	15
Criterion for Stability.....	16
HF RF vs. Microwave Stability.....	19
CHAPTER 2	
PLASMA SYSTEM MODEL.....	22
Plasma System Model Outline.....	22
Plasma Density Model.....	23
Plasma Impedance Model.....	24
Microwave Cavity Model.....	24
Transmission Line Model.....	26
Microwave Generator w/circulator Model.....	26
Complete Simulink Plasma System Model.....	28
System Stability Plots.....	28
Stability Enhancement.....	31
CHAPTER 3	
ONE DIMENSIONAL STATE MODEL CONTROL ANALYSIS.....	34
Single First Order System Ordinary Differential Equation.....	35
Stability Analysis of the System Differential Equation.....	36
Differential Equation Modification.....	37
CHAPTER 4	
EXPERIMENTAL VERIFICATION.....	39
Description of System Hardware.....	39

Standard System Performance.....	41
Standard System Analysis.....	44
Modified System.....	45
Model Verification.....	48
CONCLUSIONS.....	52
REFERENCES.....	55

TABLE OF FIGURES

Images in this thesis are presented in color.

Figure 1: General microwave powered plasma system.....	1
Figure 2: Power-loss and power-absorbed curves for three incident powers and three cavity length. Low-pressure model $v/\omega \ll 1$. Excitation frequency and background pressure are constant. (N) equals average plasma density.....	7
Figure 3: Power delivered curves.....	12
Figure 4: Standard Smith Chart.....	13
Figure 5: Plasma Impedance Curve at the plasma.....	13
Figure 6: Plasma Impedance Curve at the input to the matching device or cavity..	14
Figure 7: Plasma Impedance Curve at Generator output	15
Figure 8: Microwave/circulator Delivered Power Surface	16
Figure 9: Plasma Impedance Curve w/Delivered Power Surface at the generator output	17
Figure 10: Microwave generator Delivered Power Surface	19
Figure 11: Delivered Power Surface of solid state HF RF generator	20
Figure 12: Stable Plasma System with High Frequency RF Generator	21
Figure 13: Plasma System Model Block Diagram	22
Figure 14: Plasma System Matlab Simulink Model	28
Figure 15: Matlab 'M' file for exercising Simulink model	29
Figure 16: Reflection Coefficient (Stability) Circle of the modeled microwave plasma system	30
Figure 17: Reflection Coefficient Circle of Microwave system with added .16 wavelength transmission line	30

Figure 18: Microwave powered plasma system with reactive offset.....	31
Figure 19: Offset = +j50 Ohms microwave Delivered Power Surface	32
Figure 20: +j50 Ohms skewed Stability Circle with .16 wavelength transmission line	32
Figure 21: +j50 Ohms skewed Stability Plot with .41 wavelength transmission line.....	33
Figure 22: Stability plot, $O_f = 0$ Ohms, $a = 5$	36
Figure 23: Stability plot, $O_f = 0$ Ohms, $0 < a < 5$	37
Figure 24: Stability plot, $a = 5$, $-80 < O_f < 80$ Ohms.....	38
Figure 25: MPDR13 Microwave Cavity	40
Figure 26: Standard system schematic	41
Figure 27: Standard system performance with generator power perturbation.....	42
Figure 28: Standard system performance with cavity height perturbation.....	43
Figure 29: Standard system differential equation, resonance/density coeff 'a' = 8.....	45
Figure 30: Modified system schematic	46
Figure 31: Modified system reactive offset	46
Figure 32: Determining effective reactive offset	47
Figure 33: Modified system differential equation, $a = 8$, $O_f = -110$ Ohms.....	48
Figure 34: Modified system performance with generator power perturbation	49
Figure 35: Modified system performance with cavity height perturbation	50
Figure 36: Modified system differential equation with $1/4 \lambda$ shorter transmission line	50
Figure 37: Modified system performance with $1/4 \lambda$ shorter transmission line.....	51

INTRODUCTION

A general microwave powered plasma system is represented by Figure 1 below.

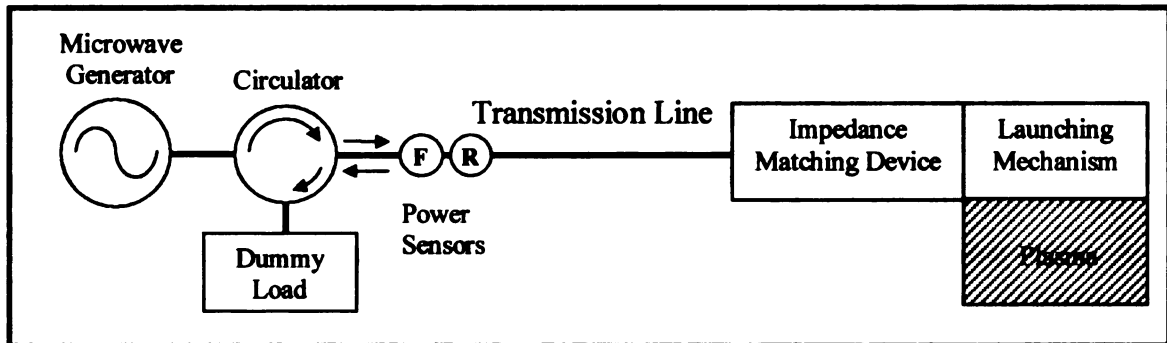


Figure 1: General microwave powered plasma system

A typical microwave generator is comprised of a high voltage DC power supply driving an output device such as a cavity magnetron or traveling wave tube (TWT). A circulator is used at the output of the generator to protect the output device from reflected energy, (mismatch), which could cause a shortened device lifetime and unstable operation, such as a shift in output frequency. A necessary component required with the use of a circulator is a matched or 'dummy' load, which the circulator directs any reflected energy to. Directional couplers placed along the transmission line are used to measure forward (F) power to and reflected (R) power from the load.

Since it is often physically inconvenient to locate a bulky microwave generator directly at the plasma source, it is common practice to use a transmission line to deliver the microwave energy to the source.

Since a plasma is not a fixed impedance energy load, an impedance matching device is required to facilitate maximal transfer of energy from the generator to the plasma. The impedance matching device can be an integral part of the launching mechanism as in a cavity type plasma source, or a general two or three stub tuning device placed along the transmission line near the radiating launching mechanism.

The term launching mechanism refers to the structure that presents the electromagnetic fields to the plasma. Some examples are: parallel plate, solenoidal coil, resonant cavity, toroidal coil, wave guide aperture, and stub antenna. How electromagnetic fields are presented to plasmas play important roles in process performance parameters such as process uniformity and process rate.

This thesis will focus mainly on a microwave cavity type plasma source though the analysis concepts will be presented in light of and are directly applicable to electromagnetic energy generated plasma sources in general, regardless of frequency or launching mechanism.

Motivations

In practice, plasma system instabilities abound, especially in plasma processing equipment operating at low-pressure regimes or with highly coupled source designs. One manifestation of this instability can make it impossible to adjust the impedance matching mechanism to obtain optimum energy transfer without extinguishing the plasma [1]. In another manifestation, especially when the output forward power of the generator is actively controlled, the amplitudes of the RF energy and/or plasma density oscillate periodically [2], often on the order of 10^3 to 10^6 Hz.

Though the need to control absorbed power in the plasma system to maintain process repeatability is somewhat obvious, there are also important motivations for minimizing reflected energy from the matching device/launching mechanism/plasma, (other than efficiency reasons). For high frequency RF (HF RF) plasma sources, harmonics of applied RF energies are generated due to the nonlinear characteristics of the

plasma. This implies that the plasma itself is an effective RF generator at these harmonic frequencies. How this effective RF generator is 'loaded' by the impedance looking back into the launching mechanism/impedance transformation device can affect several parameters of the plasma itself. The most repeatable processing is accomplished when the plasma has repeatable 'harmonic loading'. For microwave cavity type plasma sources, the mechanical structure of the cavity directly affects the electric and magnetic fields incident upon the plasma, affecting the uniformity and density profiles of the electrons, ions, radicals, etc. At any appreciable given reflected power from the cavity, there could potentially be many cavity mechanical positions, even keeping within the same resonance. This means that a plasma process could yield different rate/uniformity results for a given fixed amount of reflected power depending upon how the cavity is positioned or 'tuned'.

To summarize, an unstable RF plasma system often causes non-repeatable plasma processing. The RF/microwave power delivered to the plasma directly affects plasma density, and the impedance matching device usually affects other plasma parameters in addition to providing a means for coupling energy to the plasma. If measuring forward and reflected RF power are the only 'diagnostic' means for maintaining repeatable plasma densities, it is imperative that the reflected power be brought to a minimum by the matching device for optimum process repeatability.

Goals

The goals of this thesis are to:

- Define stability as it applies to RF/microwave driven plasma processing systems.

- Give a brief background through a summary of a previous stability analysis.
- Introduce 2 and 3-dimensional Smith plots as aids for illustrating system stability.
- Develop mathematical models of each system component.
- Develop a Matlab Simulink model of a plasma system for stability analysis.
- Using the Matlab Simulink plasma system model, show how modifying an RF/microwave generator's source impedance modifies plasma system stability.
- Describe system stability for a microwave plasma system through a single first order differential equation.
- Experimentally justify the model and control analysis through the experimental implementation of a 'stability enhanced' microwave plasma system.

CHAPTER 1 STABILITY ANALYSIS

Definition of Stability

For the purposes of this thesis, stability is defined as the ability to repeatably control plasma density through control of the RF/microwave power generator used to create the plasma. A highly stable plasma system allows the user to repeatably create and maintain a plasma at any desired density over various operating parameters of pressure, gas composition, etc... The word 'repeatably' implies at a minimum:

1. The delivered RF power to the plasma system can be repeated.

In this analysis, forward RF/microwave power is a major control input, defined as a nominal forward RF power setpoint, measured (external or internal) at the output of the RF generator. Delivered RF power is defined as the difference between this forward RF power and reflected RF/microwave power due to an impedance mismatch, (also measured at the output of the RF/microwave generator). Delivered power encompasses the losses in the transmission line, impedance matching device, launching mechanism, and most importantly, power absorbed by the plasma.

2. The transformation from the plasma impedance to the desired RF/microwave generator nominal operating impedance (typically 50 ohms) can be repeated.

Unless the system has a means for accurately measuring the impedance transformation via measuring the plasma impedance or precisely modeling the details of the transformation hardware, this second requirement for stability is difficult to achieve if the reflected power is an appreciable fraction of forward power. Only at low or zero reflected power can a repeatable transformation to the

plasma impedance be achieved. If the reflected power into the impedance matching/plasma device is high, it becomes very difficult to know to what impedance the device is transforming to. A constant standing wave ratio (SWR) describes a circle on a Smith Chart. This means that there are several impedance transformation solutions, which will yield the same SWR, whereas there is only one solution at zero reflected power.

In summary, a plasma system is stable if RF delivered power can be maintained at continuously variable levels while also reaching and maintaining low reflected power levels.

Stability Quantified

The degree of stability represents the degree to which the plasma system can be perturbed before control of the system is lost. This analysis will quantify stability by graphical means utilizing Smith Charts. The Smith Chart plots will show, for a given plasma system, areas of stable and unstable operating conditions, where the nominal center impedance represents zero reflected power from a point of view at the RF/microwave energy source, looking into transmission line towards the plasma load. The plots will also define a quantifiable measure of stability by representing the maximum stable operating region with a maximum reflection coefficient. The second stability analysis through system differential equation plotting will yield a quantifiable 'Region of Attraction' to the desired stable operating plasma density.

Background

Previous analyses of plasma system stability have utilized graphical methods to describe and explain the mechanism of cavity type source instabilities. A plot of one of these analyses [3] is recreated in Figure 2 below. The y-axis represents power absorbed/lost by the plasma and the x-axis represents plasma density. Two intersecting curves are traced on the same plot, a power loss curve and a power absorbed curve. (This thesis will use n_0 to denote plasma density and the plot below uses $\langle N \rangle$)

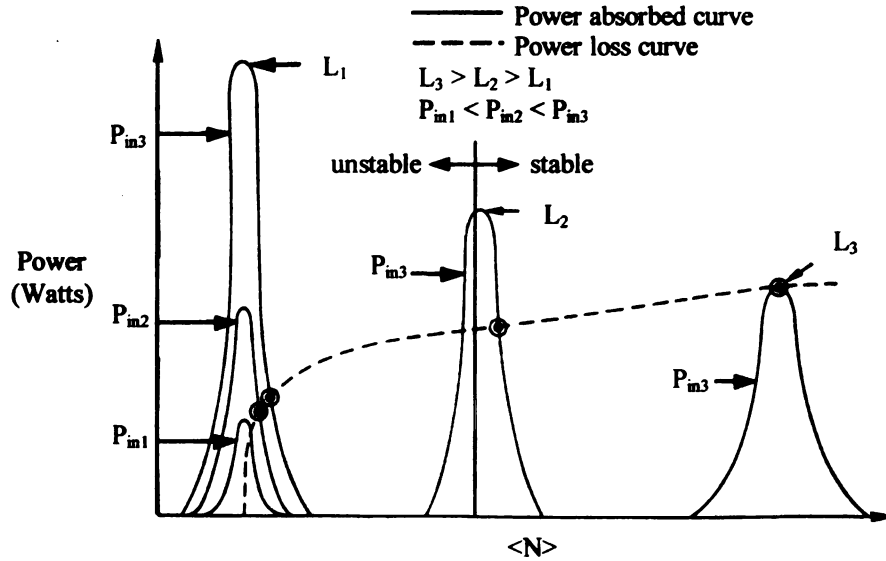


Figure 2: Power-loss and power-absorbed curves for three incident powers and three cavity lengths. Low-pressure model $v/\omega \ll 1$. Excitation frequency and background pressure are constant. $\langle N \rangle$ equals average plasma density

The power loss curve, (dotted line), represents plasma density, n_0 , as a function of power lost to the plasma, P_{loss} . In the simplest case, n_0 is approximately linearly proportional to P_{loss} with a proportionality constant $1/k_L$, where k_L is the slope of the curve in W/cm^3 .

The power absorbed curve, (solid line), represents power absorbed by the plasma, P_{abs} , as a function of plasma density n_0 . Power absorbed is dependent upon n_0 because the electrical plasma impedance changes with the density of charge carriers, n_0 , which affects the resonance or impedance transformation of whatever launching mechanism/matching network is utilized. The three curves labeled P_{in1} , P_{in2} , and P_{in3} represent three different incident power levels. This shows the effect incident power has upon the curve shapes. The three curves, (L_1 , L_2 , L_3), shown in the above figure representing three different cavity resonant modes of operation.

Changes in n_0 also affects other plasma parameters, such as sheath thickness and mobility, that can change the complex part of the electrical impedance. As the plasma impedance changes, power delivered to the plasma is affected due to changes in resonance of the cavity or matching device, affecting actual power transfer. The slope at any point along any of the P_{abs} vs. n_0 curves, we will assign as k_A , which is also in W/cm^3 . For the analysis of this thesis, it will be assumed that only one resonant mode of operation exists.

It is stated within this previous description that, “the system has solutions where the curves intersect and the system is stable if, at these points, the slope of the power absorbed curve is less than the slope of the power loss curve”. So, for the plot above, solutions along the right side of the peaks will be stable and solutions to the left are unstable if the power absorbed curve is steeper than the power loss curve. This is indicated in the plot above on the second ‘peak’. Notice that the line demarking stability is slightly offset to the left, where the slope of the power absorbed curves equals that of the power loss curve. This criterion for stability can be justified through a simple linear

control analysis, which will also be used to establish the basic criterion for stability used for the remainder of this analysis.

We will start with a very basic expression for plasma density n_o (in m^{-3}) where $1/k_L$ is the linear loss constant and τ (in sec) is an arbitrary rate constant. This rate constant is justified because the plasma density cannot change instantaneously with absorbed power. Various plasma diffusion mechanisms will regulate this rate and it can be arbitrary for this analysis because it is assumed to be the slowest responding element of the system. The general expression for n_o is:

$$(a) \quad n_o = 1/k_L \cdot P_{abs} - \tau \, dn_o/dt$$

where k_L is the slope of the power loss curve at any solution, in Watts/ m^3 .

Then, we state that P_{abs} is a function of n_o with the agreement that at any real solution, power lost is the same as power absorbed. Also, since changes of plasma density affect absorbed power much faster than the diffusion rate constant described above, the following function is not considered to be time dependant:

$$(b) \quad P_{abs} = k_A \cdot n_o$$

where k_A is the slope at any point along whatever curve is traced by the power absorbed curve at any solution, also in Watts/ m^3 .

Substituting $k_A \cdot n_o$ for P_{abs} into equation (a) above yields:

$$(c) \quad n_o = (1/k_L \cdot k_A \cdot n_o) - \tau \, dn_o/dt$$

Solving for dn_o/dt yields:

$$(d) \quad \frac{dn_o}{dt} = \frac{n_o \cdot (k_A/k_L - 1)}{\tau}$$

This is the first order differential equation that describes the system. The equation does not need to be solved to determine stability. At any of the solutions, the system is

stable as long as the right side is negative with respect to the left side. For this equation, the system is stable when k_A / k_L is less than 1, or $k_A < k_L$. Put into words, when the right side of the equation is negative, the density n_0 will always move in the opposite direction of any perturbation to n_0 . If the right side of the equation is perturbed in a positive direction ($n_0 + dn_0$), then the motion of n_0 , which is dn_0/dt , will move in the opposite direction, regaining equilibrium. On the other hand, if the right side of the equation is positive with k_A larger than k_L , then the response dn_0/dt will be in the same direction as the perturbation resulting in a rapid movement away from equilibrium at a rate inversely proportional to the arbitrary diffusion time constant τ .

Thus, the previous descriptive criterion for stability is justified mathematically. The plasma system is stable if, for any real solution, the slope of the power absorbed curve, k_A , is less than the slope of the power loss curve, k_L .

Definition of Variables

While it is immediately understood that plasma density, n_0 , is some function of power lost to the plasma, it may not be as clear that absorbed power, P_{abs} , is some function of plasma density without the auxiliary parameter of plasma impedance, Z_p . Since plasma density is directly related to charge carrier density, it is a small step to conclude that the real part, R_p , of plasma impedance, Z_p , is inversely proportional to n_0 . Furthermore, since n_0 affects other plasma parameters such as sheath thickness and carrier mobility, the reactive part, X_p , of plasma impedance Z_p is also some function of n_0 . Now that we have plasma impedance, Z_p , as some function of n_0 , it is easily understood that the operating resonance of the launching mechanism and thus, the

effective energy transfer is some function n_0 . Thus, the amount of reflected power from this matching device/launching mechanism mismatch is some function of n_0 . Lastly, these changes in reflected RF power directly equates to changes in ‘Delivered’ RF power through some relation of the ability of the generator to deliver power as a function of reflected RF power, P_{rf} , and thus as a function of n_0 . Viewing this sequence using plasma impedance, it is easier to see how changes to n_0 affect absorbed power which is the same as delivered power, P_{del} , if we neglect the losses outside of the plasma.

Let us now shift our frame of reference from plasma density, n_0 , to plasma impedance, Z_p , and secondly, from P_{abs} & P_{loss} to the single term, Delivered Power P_{del} . Since there are only real solutions in a real system, we don’t need to distinguish between P_{abs} and P_{loss} , and we agree that the power used by the plasma is the same as power delivered, P_{del} , to the plasma which is also the same as forward power, P_{fwd} , minus reflected power, P_{rf} , (excluding system losses outside the plasma). Now the stability analysis involves two different system equations: one relating how plasma impedance is affected by delivered power, and another relating how delivered power is affected by the plasma impedance. Making this change of variables makes it easier to understand the way the previously plotted ‘power absorbed curve’ is generated and what can affect its shape.

Focusing on just the real part, R_p , of the plasma impedance, Z_p , we can create a similar plot to Figure 2, using our new variable, P_{del} , as shown in Figure 3 below.

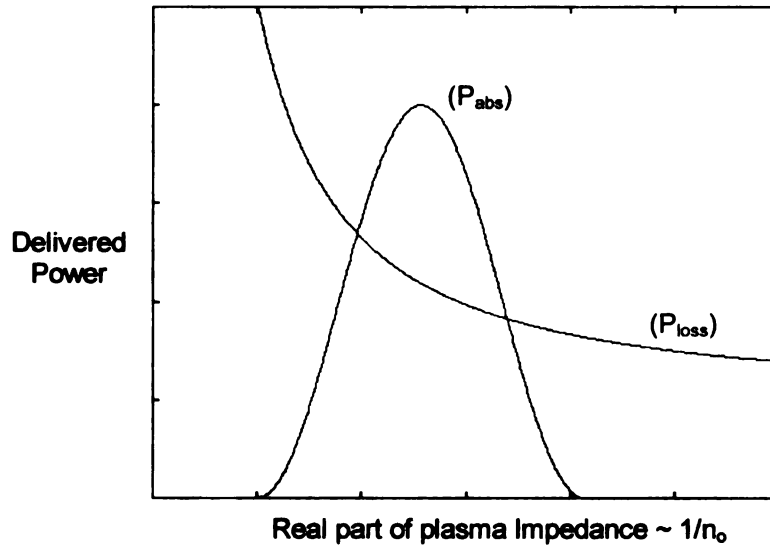


Figure 3: Power delivered curves

Plasma Impedance Curve

Because we shifted our reference to plasma impedance, Z_p , we now see that the complete picture can only be represented in 3 dimensions, where the complete plasma impedance including the real part, R_p , and reactive part X_p , are plotted against the now singly defined Delivered Power P_{del} . To increase clarity, let us use the well known Smith chart to represent plasma impedance in 2 dimensions as a bottom polar plane, with delivered power, P_{del} , as a linear vertical center axis, originating at the nominal Z_0 point of the Smith Chart. For reference, Figure 4 shows the standard (2-dimensional) Smith Chart.

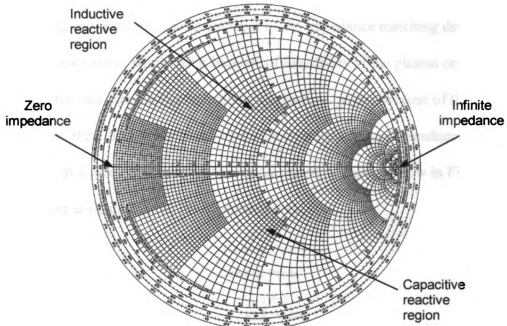


Figure 4: Standard Smith Chart

Rotating the standard Smith Chart to lay down almost flat and adding the third dimension of delivered power, we arrive at a 3-dimensional (3-D) Smith Chart. With this 3-D Smith Chart, we can now plot our first system equation in the new coordinates : Z_p vs. P_{del} defined as a Plasma Impedance Curve, with an example shown below in Figure 5, (where Z_p is inversely proportional to n_o and n_o is linearly proportional to P_{del}).

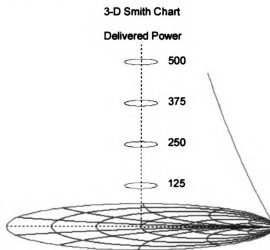


Figure 5: Plasma Impedance Curve at the plasma

Shifting our point of view to the input of the impedance matching device, the plasma impedance curve would twist because of the affects of the plasma on the resonance of the matching device/launching mechanism. Also, because of the impedance transformation, there is now a solution of the curve at the nominal impedance, (Smith Chart center), at a given delivered power. In the example shown below in Figure 6, reflected power is minimized at 300 Watts delivered.

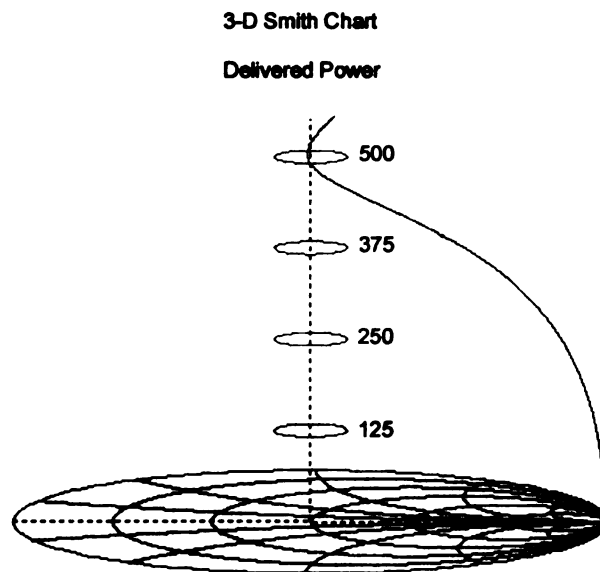


Figure 6: Plasma Impedance Curve at the input to the matching device or cavity

Shifting our point of view again down an arbitrary length transmission line to the output of the microwave generator/circulator, the plasma impedance curve arbitrarily rotates around the Smith Chart as shown below in Figure 7.

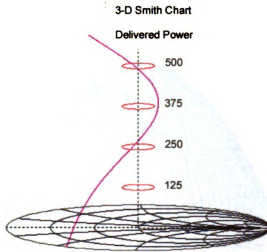


Figure 7: Plasma Impedance Curve at Generator output

This is the point of view from which the rest of this stability analysis will be made.

Delivered Power Surface

The second system equation using the defined state variables is P_{del} as a function of Z_p . This equation defines a *surface* which this thesis will define as a Delivered Power Surface. An example of such a surface viewed at the output of a typical microwave/circulator combination is shown in Figure 8 below. This is the same point of view mentioned above, at the output of the generator, looking into the transmission line towards the plasma load.

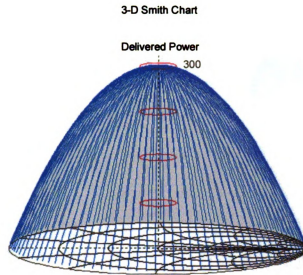


Figure 8: Microwave/circulator Delivered Power Surface

This surface represents the energy delivered by a generator versus the load impedance presented to it. For the case of a microwave generator with a circulator at its output, the equation for this surface is based on delivered power equals forward (setpoint) power minus reflected power, where the reflected power is a function of load impedance.

Criterion for Stability

Putting the plasma impedance curve together with the delivered power surface we arrive at Figure 9. The arrows indicate the two possible solutions, where the plasma impedance curve meets the delivered power surface.

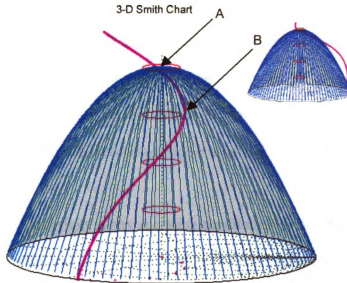


Figure 9: Plasma Impedance Curve w/Delivered Power Surface at the generator output

As the output power setpoint of the RF/microwave generator is varied, the height of the delivered power surface is affected. As the matching network or cavity is 'tuned', the height and shape of the plasma impedance curve is varied. As the length of the transmission line is varied, the radial orientation of the plasma impedance curve is varied. For Figure 9 above, radial orientation does not affect the apparent 'solutions' of the curve and surface because the surface is radially symmetric about the nominal impedance. The inset in the upper right is the same surface and curve but rotated 90 degrees CCW to show that the plasma impedance curve is indeed outside of the surface up until it enters the surface at point B.

Similar to the preceding 2-dimensional stability analysis, intersecting points of the plasma impedance curve to the delivered power surface define real solutions of the plasma system. The criterion for stability requires that the slope of the surface tangent (in the direction of the curve tangent) is less than the slope of the curve tangent. If, at the

intersection, the tangent slope of the delivered power surface (in the curve direction) is steeper than the tangent slope of the plasma impedance curve then the solution is unstable. Using Figure 9 above, the intersecting solution at point 'A' of the plot is stable (surface slope is zero in direction of curve), and the intersecting point at point 'B' of the figure is unstable (surface slope in direction of curve is greater (steeper) than curve slope).

We will define equilibrium as any operating condition in which RF energy is being delivered to a plasma, and the state variables of delivered power and the plasma impedance are not changing with respect to time. The extent to which a system at equilibrium can be perturbed and still return to equilibrium is quantifiable, where a high degree of allowed perturbation about the desired operating point is considered to be a desirable attribute of a plasma processing system.

In Figure 9 above, the matching network or cavity is set to bring a solution to low reflected power, point A. It is now clearly seen that if the system is perturbed in such a way as to raise the plasma impedance curve slightly, a marginally stable operating point quickly becomes the only solution and the plasma soon extinguishes. If, however, the system is perturbed so as to lower the curve, the system remains stable for a much larger perturbation in that direction. Thus, it is important to note that the perturbation direction and magnitude that will maintain system equilibrium is not symmetric. In the case above, for some directions, a very small perturbation from the desired operating point (A) will result in loss of equilibrium.

HF RF vs. Microwave Stability

A microwave generator utilizes a circulator at it's output to both protect the power device (such as a magnetron), and to maintain output stability (mode reduction). Because of the circulator, a microwave generator has an effective nominal source impedance of 50 ohms. The delivered power surface characteristics of this microwave energy source appears as indicated by Figure 10 below.

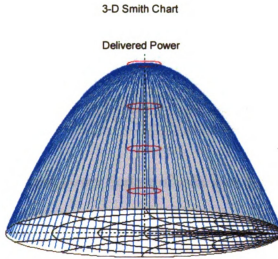


Figure 10: Microwave generator Delivered Power Surface

Typical high frequency (HF) RF generators (3 to 30 MHz) usually have a source impedance far from their nominal operating impedance of 50 ohms. The 50-ohm nominal impedance is a load for which the generator is best suited to deliver stable and efficient RF energy. They are often designed as a low impedance 'voltage source' which is then transformed to some other source impedance through harmonic filtering or output impedance matching, but still far from 50 ohms. This default design strategy has inadvertently given the HF RF generator a stability advantage for use in plasma systems

over the microwave RF generator. Figure 11 below shows a typical delivered power surface of a solid state HF RF generator.

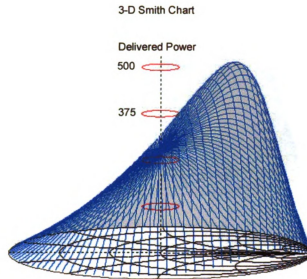


Figure 11: Delivered Power Surface of solid state HF RF generator

Because of the characteristic of a ‘voltage source’ or ‘current source’, the generator delivers much more power at some other load impedance than nominal. This is true even if there is a control loop maintaining the forward or delivered output power because the speed of that control loop is typically much slower than the speed at which the plasma impedance can respond. So for this analysis, we must consider any HF RF generator to be ‘uncontrolled’. It is now easily possible to have a stable operating point at ‘best tune’ where the plasma impedance curve meets this surface at the nominal impedance center. At this point there is no reflected power, and a relatively large perturbation in any direction will not cause loss of equilibrium. The same plasma impedance curve is introduced onto the HF RF delivered power surface in Figure 12 below.

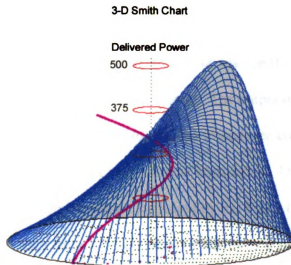


Figure 12: Stable Plasma System with High Frequency RF Generator

Note also that the system stability is now dependant upon choosing a transmission line length that rotates the plasma impedance curve into the position where it's slope is in the opposite direction as the slope of the tangent plane of the delivered power surface. Thus, the stability of this system is now transmission line length dependant because the delivered power surface is no longer symmetric about the nominal axis.

If a microwave generator could be modified to have an asymmetric output power surface similar to that of an HF RF generator, the same stability could be effected. This will be attempted and shown subsequently in the system model with the results shown on 'stability region' plots.

CHAPTER 2 PLASMA SYSTEM MODEL

We will now utilize a Simulink model to further analyze the stability characteristics of a typical microwave plasma system. The output of the model is a 2-dimensional Smith chart of the solution of the plasma impedance curve and the delivered power surface, given different ‘starting’ positions of impedance. The charts will show regions of stable solutions. The impedance indicated by the Smith Chart stability plots will be the impedance as seen from our view point of just outside of the RF generator, looking into the transmission line.

We will also use the model to see how the system can be modified to maximize the degree of stability as previously defined.

Plasma System Model Outline

Figure 13 below is a block diagram to represent the various pieces of the plasma system model to be developed. Each block will be represented by the functions indicated in the blocks and the functions themselves will be defined. Then the individual functions will be ‘connected’ together as shown in the figure in the form of a Matlab Simulink model.

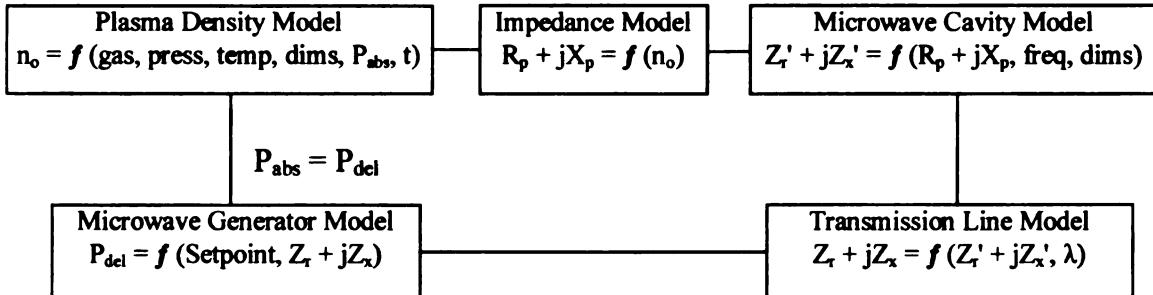


Figure 13: Plasma System Model Block Diagram

Plasma Density Model

The form of the plasma density model used is based upon energy balance equations for electropositive plasmas in equilibrium [4]. This form is:

$$n_o = k_L P_{abs}(n_o)$$

where n_o is plasma density, P_{abs} is absorbed power, and k_L is the plasma load line constant which absorbs all process parameters such as gas, pressure, temperature, etc. This is a linear proportionality constant relating plasma density to absorbed power. A second term is added to represent a time dependence of plasma density to changes in absorbed power, with τ being an arbitrary time constant:

$$n_o = k_L P_{abs}(n_o) - \tau \frac{dn_o}{dt}$$

Based upon previous data taken for the MPDR13 plasma reactor [5], (to be used to verify the model), the plasma load line constant was chosen which yielded a plasma density of $4.4 \times 10^{17} \text{ m}^{-3}$ for 200 Watts of absorbed power:

$$k_L = 2.2 \times 10^{15} \text{ W}^{-1} \text{ m}^{-3}$$

An arbitrarily picked ionization time constant was chosen which represented a conceivable average time between ionizations. Since this is the only, (and therefore dominant), time constant for the whole system, it can be arbitrary. Also, the transient response of the system is not being investigated, only the stability:

$$\tau = 1 / \nu_{iz} = 3.13 \times 10^{-5} \text{ s}$$

Solving the plasma density equation for dn_o/dt yields the ordinary differential equation for the system:

- $$\frac{dn_o}{dt} = \frac{P_{abs}(n_o) k_L}{\tau} - \frac{n_o}{\tau}$$

*Assumptions: Plasma density is linearly proportional to P_{abs} .
Plasma density time constant is arbitrary and possibly related to ionization rate.*

Plasma Impedance Model

Plasma impedance Z_p can be defined by the series representation:

$$Z_p = R_p + j X_p$$

As a function of plasma density n_0 , the real part of the plasma impedance, R_p , is inversely proportional to conductivity which therefore makes it inversely proportional to charge carrier density, hence inversely proportional to n_0 .

- $R_p = \frac{k_r}{(n_0 + \text{Cavity Losses})}$

Where k_r is an arbitrary proportionality constant and ‘Cavity Losses’ is a term introduced for the purpose of eliminating the zero plasma density singularity:

$$\text{Cavity Losses} = 1 \text{ E16}$$

The reactive part of the plasma impedance will be ignored, as it will be absorbed into the relation of plasma density to cavity resonance, later in the model:

- $X_p = 0$

Assumptions: There is a linear relationship between plasma conductivity and density, with no appreciable reactive element.

Microwave Cavity Model

At the desired operating point, the microwave cavity transforms the real part of the plasma impedance to the nominal transmission line impedance, Z_0 , of 50 ohms:

$$Z_r' = k_l * R_p$$

$$Z_r' = \frac{k_l}{(n_0 + \text{Cavity Losses})}$$

where Z_r' is the real part of the impedance Z' looking into cavity from the driving point and k_1 is the proportionality constant, (absorbs k_r), that represents the impedance transformation. For this model, k_1 is chosen to make $R_p' = 50$ ohms at the desired operating point:

$$k_1 = 2.25 \text{ E}19 \quad \text{at } P_{\text{abs}} = 200\text{W}, \text{ and } n_0 = 4.4\text{E}17$$

An term is added, (in brackets), to represent changes to the real part, Z_r' , as an arbitrary function of cavity probe height h_p . Cavity excitation probe height h_p is normalized to a value of 50 (Z_0). This will be used to perturb the real part Z_r' :

$$\bullet \quad Z_r' = \frac{k_1 * [5 \wedge ((h_p - Z_0) / Z_0)]}{(n_0 + \text{Cavity Losses})}$$

Assumptions: The approximate model is based upon observed probe height vs. SWR data.

The reactive part (Z_x') of the impedance looking into cavity from driving point as a function of real part of plasma impedance R_p can be represented by:

$$Z_x' = a * R_p$$

where constant 'a' is a linear scaling factor representing the degree to which a changing plasma density affects cavity resonance. This term also absorbs any reactive part of the plasma itself as previously mentioned. A value of 5 was used for the analysis and plots above, such as in Figure 9. This value was somewhat randomly chosen for illustration purposes and will later be adjusted to model actual observed cavity performance.

Assumptions: Cavity resonance is inversely affected by plasma density, possibly due to change of sheath thickness [6] and conductive medium (plasma) skin depth [7].

Including another term to account for the effects of cavity height h_c on cavity resonance, and hence, perturb the reactive part of the impedance, gives:

- $Z_x' = a * (R_p - h_c)$

where h_c is normalized to R_p nominal (Z_0).

Assumptions: The dependence of Z_x' on h_c model is approximately based upon observed density and cavity height versus SWR data.

Transmission Line Model

Standard lossless transmission line equations [8], transform the impedance looking into the cavity Z' into the impedance $Z = Z_r + jZ_x$ looking into a λ -wavelengths long, Z_0 Ohm transmission line via the following development:

$$\Gamma_v = (Z_r' + jZ_x' - Z_0) / (Z_r' + jZ_x' + Z_0) \text{ (Voltage Reflection coefficient)}$$

$$R_x = (\Gamma_v \cos(2\lambda) - 1) / 2$$

$$R_y = \Gamma_v \sin(2\lambda) / 2$$

- $Z_r = \frac{Z_0}{\frac{R_y'^2}{\text{abs}(R_x)} - R_x} - Z_0$

- $Z_x = \frac{(Z_0 R_y)}{\frac{(R_x R_y')}{\text{abs}(R_x)} - R_x^2}$

Assumptions: The transmission line is lossless.

Microwave Generator w/circulator Model

Since there is a circulator connected at the output of the microwave generator, the delivered power, P_{del} , is a function of reflected power, P_{rf} , and is given by:

$$P_{del} = P_{fwd} - P_{rf}$$

where P_{fwd} is the generator setpoint or incident power, often automatically controlled, but in the experimental case later outlined, manually set.

Reflected Power P_{ref} for a given power reflection coefficient Γ_p , at a given forward power P_{fwd} is given by:

$$P_{\text{ref}} = P_{\text{fwd}} * \Gamma_p$$

where the power reflection coefficient Γ_p is defined as:

$$\Gamma_p = ((Z_r + jZ_x - Z_0)^2 / (Z_r + jZ_x + Z_0)^2)$$

where Z_0 is the nominal impedance and $Z_r + jZ_x$ is the impedance looking into the transmission line towards the load.

Writing in terms of delivered power P_{del} defined above:

$$P_{\text{del}} = P_{\text{fwd}} - (P_{\text{fwd}} * \Gamma_p)$$

$$P_{\text{del}} = P_{\text{fwd}} * (1 - \Gamma_p)$$

The complete microwave generator w/circulator model relating delivered output power P_{del} as a function of Setpoint Power P_{set} , nominal impedance Z_0 , and load impedance $Z_r + jZ_x$ (as seen by RF Generator's circulator output) can now be written as:

$$P_{\text{del}} = P_{\text{set}} * [1 - (Z_r + jZ_x - Z_0)^2 / (Z_r + jZ_x + Z_0)^2]$$

where P_{set} is the forward setpoint control input, taking the place of P_{fwd} .

Because imaginary terms cannot be modeled directly in Matlab Simulink, the equation is rewritten in terms of magnitudes, yielding:

- $P_{\text{del}} = P_{\text{set}} * [1 - ((Z_r - Z_0)^2 + Z_x^2) / ((Z_r + Z_0)^2 + Z_x^2)]$

Assumptions: The circulator is ideal and lossless.

Complete Simulink Plasma System Model:

The preceding model components were brought together into a single Matlab Simulink model shown below in Figure 14. The blocks of Figure 13 are shown with dashed lines on the Simulink model. The Transmission Line Model is shown as a simplified single block comprised of a Matlab Subsystem for ease of readability.

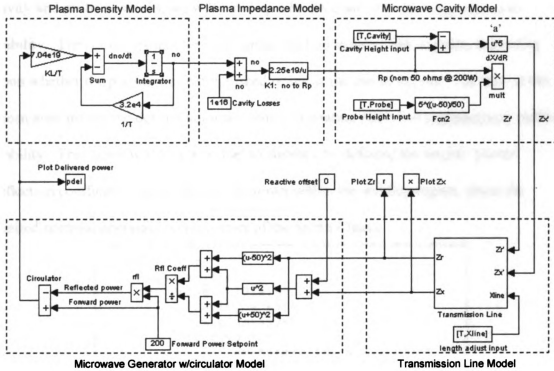


Figure 14: Plasma System Matlab Simulink Model

System Stability Plots

The Simulink model will be used to show operating parameter 'regions of stability'. In this case, the operating parameters that are being tracked $r + jx$ (complex impedance) as seen from the output of the microwave source, looking into the transmission line towards the plasma load. The starting plasma density is preset to a nominal value, as if the modifiable parameters of cavity height and cavity probe height

are at optimum positions. Then, a Matlab 'M' file, (Figure 15 below), is used to manipulate cavity and probe height positions and run the system model to track the progression of the system parameters of impedance ($r + jx$) over time. A stable condition results in $r + jx$ moving to some impedance other than purely reactive, (which would indicate that the plasma has extinguished). If we then repeat the simulation for different cavity and probe positions, we will build up a Smith Chart plot showing regions of stability. The starting points for each run are plotted in either red or green, depending upon whether the plasma was extinguished or not at the end of the run. The size of the green area around the desired nominal 'center' operating point will quantitatively define stability. This thesis will give a 'value' to stability by defining the largest 'power reflection coefficient' circle that can be drawn within the stability region, about the desired nominal operating point, (center of the Smith Chart).

```

hold off
Xline = .16;
for Probe = 10:4:90
    for Cavity = 65:-.5:35
        sim plasmasys
        if r(500) < 5
            smithrx(r(1), x(1), 'r*')
        elseif r(500) > 500
            smithrx(r(1), x(1), 'r*')
        else
            smithrx(r(1), x(1), 'g*')
        end
        hold on
    end
end
end

```

Figure 15: Matlab 'M' file for exercising Simulink model

Figure 16 below is a run utilizing an ideal microwave energy source as indicated by the delivered power surface of Figure 10. The largest power reflection coefficient circle that can be drawn in the stable region is .02. Thus, the larger the allowed reflection coefficient, the more the system can be perturbed in any direction without going unstable.

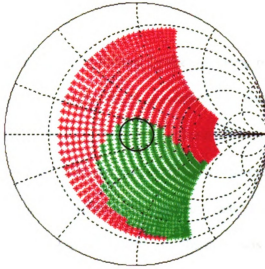


Figure 16: Reflection Coefficient (Stability) Circle of the modeled microwave plasma system

If the length of the transmission line is changed as indicated in Figure 17 below, the maximum allowed reflection coefficient does not change due to the symmetry of the microwave generator delivered power surface, (Figure 10).

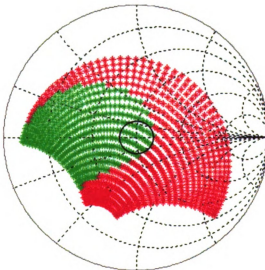


Figure 17: Reflection Coefficient Circle of Microwave system with added .16 wavelength transmission line

Stability Enhancement

The plasma impedance curve is defined by the operating parameters of the plasma and plasma source such as pressure, chemistry, geometry, etc, and the electrical characteristics of the transmission line, matching device and launching mechanism. The delivered power surface, up until now, has been defined by the electrical characteristics of an 'ideal' microwave energy source with an output circulator. Since the plasma impedance curve is often mostly a given, defined by the demands of a plasma process, plasma chamber design, and launching mechanism, we are left with the delivered power surface and transmission line to modify, in an attempt to increase a system's stability.

If we now introduce a reactive offset element placed between the microwave output and it's circulator, we can skew the microwave generator's delivered power surface. A block diagram of this modified system is indicated below in Figure 18.

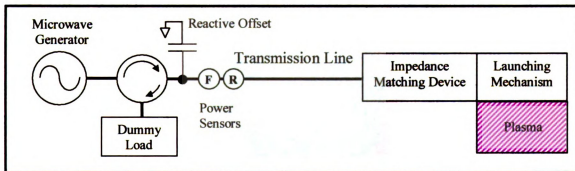


Figure 18: Microwave powered plasma system with reactive offset

A 'reactive offset' input can also be seen in the complete Simulink model of Figure 14. The offset creates a similar delivered power surface to the HF RF powered system described above with Figure 11, and is shown below in Figure 19.

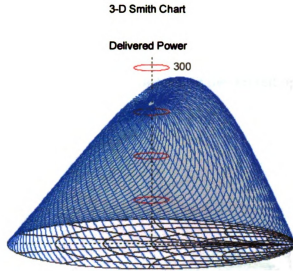


Figure 19: Offset = $+j50$ Ohms microwave Delivered Power Surface

The resulting Simulink stability run now shows a greatly increased allowed reflection coefficient of about .3 as shown in Figure 20 below.

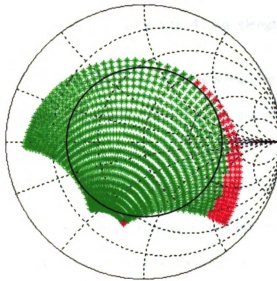


Figure 20: $+j50$ Ohms skewed Stability Circle with .16 wavelength transmission line

As in the HF RF power system, the new system with a skewed delivered power surface has now become dependant upon the transmission line length for it's stability.

This is illustrated in Figure 21 below. This is the exact system as indicated above in Figure 18 with the reactive offset, except the transmission line was increased and extra 1/4 wavelength. The system is completely unstable at the desired operating point.

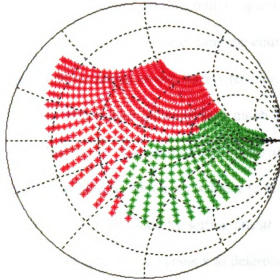


Figure 21: +j50 Ohms skewed Stability Plot with .41 wavelength transmission line

The disadvantage of using this method of adding a reactive offset is that when the cavity is positioned for best tune and reflected power is low, the impedance looking into the offset from the point of view at the output of the circulator is not 50 ohms. This means that the reflected energy due to this mismatch is dumped into the dummy load connected to the third port of the circulator. During normal operation, efficiency is not maximized, and the microwave generator must be chosen to be able to provide more energy than required by the plasma process.

CHAPTER 3

ONE DIMENSIONAL STATE MODEL CONTROL ANALYSIS

Analyzing the stability of the plasma system can also be accomplished by observing the zeros and plots of the single first order differential equation that describes the system. For a first order system, solving the differential equation is not required to observe its exact response. It is enough to first determine the equilibrium points, and then determine whether the points are stable or not, then determine the 'Region of Attraction' for the stable points. This region indicates how much the system can be perturbed before it loses equilibrium [9]. The equilibrium points are the conditions which lead to zero motion of the state variable, x , which we will use to represent plasma density n_0 . The equilibrium points are easily determined by setting $dn_0/dt = 0$ ($x' = 0$), then solving for x . The next step is to simply plot x' versus x to determine the region of attraction to the stable equilibrium points. For this system, we will find 2 stable equilibrium points and one unstable point. If the plasma density is perturbed from the stable to the unstable equilibrium point, the system state will transit to the third equilibrium point which we will find to be at zero density, representing an extinguishment of the plasma.

We must first build the whole differential equation for the system using the component models already developed. Since we wish to observe the effects of the introduced reactive offset and the effects of plasma density on cavity resonance, we will carry these variables all the way through to the final equation. The equations for the transmission line will be neglected as they would greatly increase the complexity of the differential equation. Because of this, choosing the polarity of the reactive offset (capacitive or inductive) will lead to either a more stable or less stable system. The

transmission line in a real system gives added flexibility for gaining stability at either polarity.

Single First Order System Ordinary Differential Equation

Starting with the original first order differential equation of the system:

$$dn_o/dt = P_{del}(n_o) k_L / \tau - n_o / \tau$$

Letting :

$$x = n_o$$

$$x' = dn_o/dt$$

$$A = k_L / \tau = 7.04e19$$

$$B = 1 / \tau = 3.20e4$$

$$P_{del}(n_o) = P(x)$$

$$\bullet \quad x' = AP(x) - Bx$$

The function $P(x)$ is the delivered power as a function of plasma density. Starting with P as a function of impedance:

$$P(Z_r, Z_x) = P_{set} * [1 - ((Z_r - Z_o)^2 + Z_x^2) / ((Z_r + Z_o)^2 + Z_x^2)]$$

Letting :

$$P_{set} = 200$$

$$Z_r = k_1 / n_o$$

$$Z_o = 50 \text{ (nominal impedance)}$$

$$Z_x = a * ((k_1 / n_o) - Z_o) + O_f$$

$$k_1 = 2.25e19$$

$$O_f = \text{Reactive Offset in Ohms}$$

where 'a' represents the effect of plasma density on system resonance and O_f represents the introduced reactive offset.

Rewriting $P(Z_r, Z_x)$ as $P(x)$:

$$P(Z_r, Z_x) = P_{set} \cdot \left[1 - \frac{((Z_r - Z_o)^2 + Z_x^2)}{((Z_r + Z_o)^2 + Z_x^2)} \right]$$

$$P(x) = P_{set} \cdot \left[1 - \frac{(k_1/x - 50)^2 + (a k_1/x - 50a + O_f)^2}{(k_1/x + 50)^2 + (a k_1/x - 50a + O_f)^2} \right]$$

Writing $P(x)$ into the differential equation above yields (1):

$$x' = \frac{[100BaO_f - 2500B(1+a^2) - BO_f^2]x^3 - [100Bk_1(1-a^2) + 2Bak_1O_f]x^2 + [200Ak_1P_{set} - Bk_1^2(1+a^2)]x}{[2500(1+a^2) - 100aO_f + O_f^2]x^2 + [100k_1(1-a^2) + 2ak_1O_f]x + [k_1^2(1+a^2)]}$$

Stability Analysis of the System Differential Equation

Setting x' to zero yields the equilibrium points for plasma density x . Setting the density/resonance constant ' a ' above to 5, with no reactive offset, ($O_f = 0$ Ohms), then solving the 3rd order polynomial of the numerator above yields three roots or equilibrium points: 0, $3.7e17$, and $4.4e17$. Plotting the curve of plasma density motion (x') versus plasma density (x) below in Figure 22 shows these three equilibrium points.

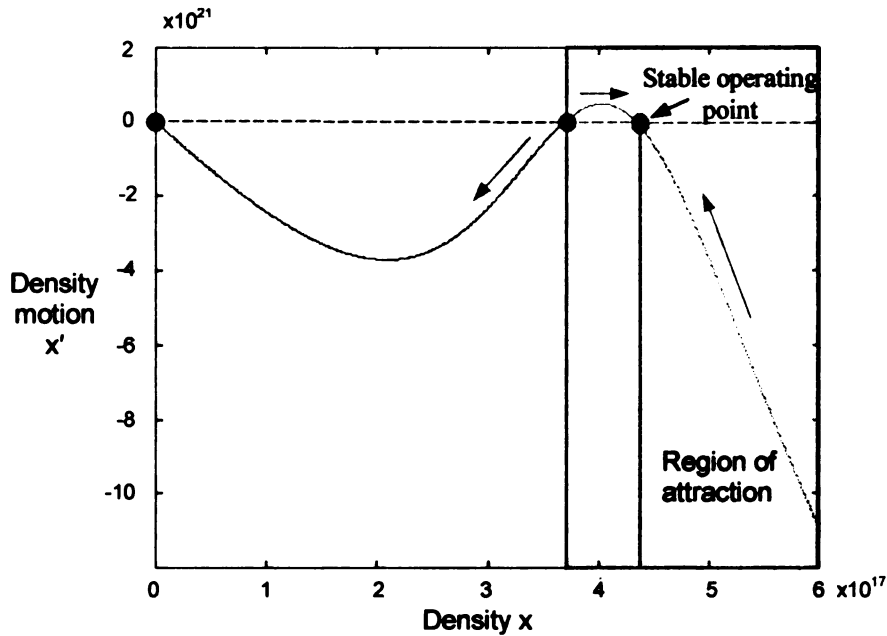


Figure 22: Stability plot, $O_f = 0$ Ohms, $a = 5$

The stability of each equilibrium point is tested by observing the slope of the trajectory at the point. A negative slope indicates an asymptotically stable point and a positive slope is an unstable point. Thus the equilibrium points at 0 and $4.3e17$ are stable (green), and the point at $3.7e17$ is unstable (red). Any point on the line will move to the

right if the point is positive in the x' direction (vertical axis), and will move to the left if the point is negative in the x' direction. Thus, as long as the operating conditions yield a plasma density above $3.7\text{e}17$, the system will move to the stable operating point, $4.4\text{e}17$. This is the region of attraction for the system and is shown shaded in green. If the system is perturbed to the point where plasma density drops below $3.7\text{e}17$, the system will transit to the other equilibrium point, zero, at a rate governed by plasma diffusion mechanisms, and the plasma is extinguished. Thus the 'region of attraction' is from plasma densities of $3.7\text{e}17\text{ m}^{-3}$ and up. By observation, this region is not symmetrical, and it would be desirable to increase the narrow left side to allow for larger system perturbations.

Differential Equation Modification

The system differential equation can now be modified to observe the resultant regions of attraction, and thus changes to stability. A family of curves is generated below in Figure 23, by varying the density/resonance constant ' a ' from 0 to 5.

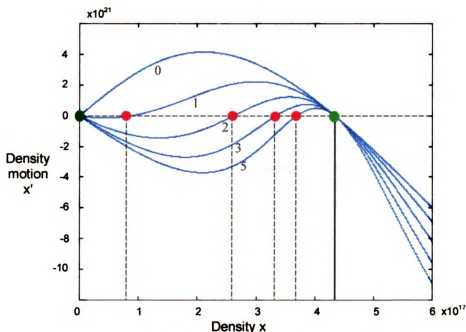


Figure 23: Stability plot, $O_r = 0$ Ohms, $0 < a < 5$

It can be immediately concluded by this family of curves that decreasing the effect plasma density has on the resonance of the cavity greatly increases the system region of attraction to the desired stable operating point. Leaving 'a' set to 5, another family of curves shown below in Figure 24 is generated by allowing the reactive offset, O_f , vary from -80 to 80 Ohms.

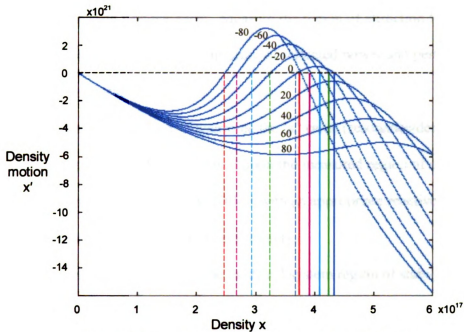


Figure 24: Stability plot, $a = 5$, $-80 < O_f < 80$ Ohms

It is observed by the family of curves above that the region of attraction can be completely cutoff for the desired equilibrium point for positive reactive offsets. A substantial gain in stability region is observed, (distance between similar colored equilibrium points), for negative reactive offsets, along with a corresponding small shift in the stable equilibrium point.

CHAPTER 4 EXPERIMENTAL VERIFICATION

Verification of the system model was obtained through the use of an MPDR13, (Microwave Plasma Disk Reactor) plasma system [10]. The goal will be to justify the effectiveness of using a simple first order system differential equation for the purpose of predicting and assessing system stability. Verification will be performed in four steps:

1. *Standard system performance:* Measure the region of attraction for the standard MPDR13 through monitoring of reflected power and perturbing the system into instability.
2. *Standard system analysis:* Determine the 'a' value (resonance/density coefficient) for the MPDR13 based upon the measured region of attraction.
3. *Modify system:* Modify the MPDR13 with an appropriate reactive offset and transmission line length to increase stability.
4. *Model verification:* Measure the modified system region of stability and compare to the model predicted region of attraction.

The system will be perturbed for the verification procedure above by moving the height, (distance L_s of Fig, 25 below), of the cavity to create a mismatch. Secondly, the system will be perturbed by changing the power setpoint of the microwave generator. Percentages of power change for which the system remains stable will be compared between the modified and unmodified systems.

Description of System Hardware

Stability analysis verification was obtained with an MPDR13 microwave cavity type plasma system, as shown below in Figure 25, with general dimensions in cm.

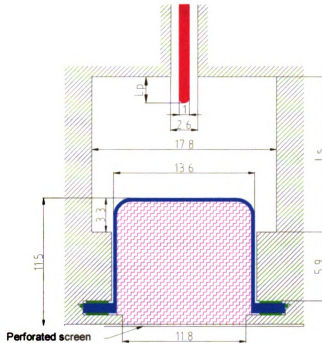


Figure 25: MPDR13 Microwave Cavity

The center fed probe (red) is excited with 2.45 GHz microwave energy, delivered via a coaxial transmission line. The cavity excitation probe (L_p) and cavity (L_s) heights are adjustable and the plasma is contained within a quartz dome shown in blue, located in the lower portion of the cavity.

For the stability analysis, Argon was used at a pressure of 500mT. At this pressure the standard system instability was less pronounced and it was possible to obtain a somewhat accurate measure of reflected power at the point of instability. This pressure required a flow rate of about 75 sccm, pumped by an Edwards Model 5, two stage mechanical pump. The cavity probe length L_p was set to 2.9 cm. The following sequence was used for all data runs to insure plasma ignition:

- The microwave generator was set to have a magnetron current of 300 ma or an indicated forward output power of 200W, whichever came first.
- The cavity height was brought to 12 cm.

- c. The cavity height was then brought up to 15 cm, followed by upward manual incremental tuning.

Standard System Performance

Figure 26 below is a schematic of the standard system used for verification.

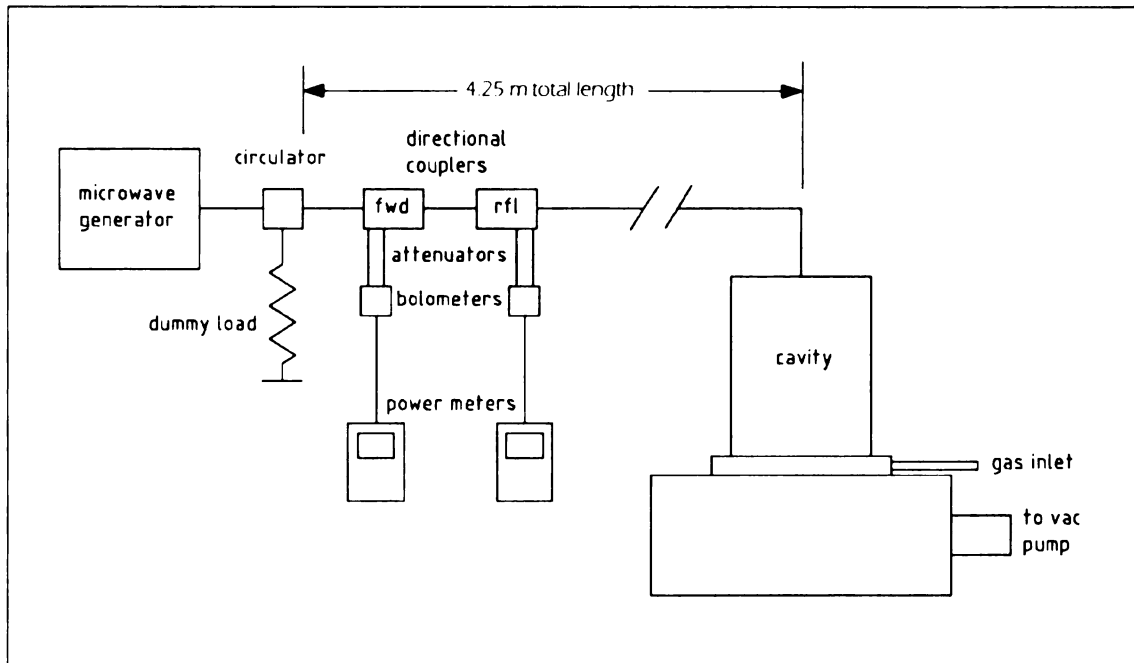


Figure 26: Standard system schematic

The microwave generator was a Micro-Now model 420B1 with a UTE Microwave model CT-3695N circulator. The directional couplers for forward and reflected power measurements were two Narda 2785-30's. Power was measured with two HP model 432A w/478A bolometer type power meters connected via two 20 db attenuators.

This standard system was run to find the maximum amount of perturbation that could be made without causing the system to go unstable. This characterization of the standard system versus power setpoint was performed by the following sequence:

1. Adjusting the cavity to a best tune position at 200 Watts incident, which was a reading of 0 to 2 Watts, (measured after the circulator).
2. Turning the generator power control to maximum power.
3. Slowly adjusting the generator's power setpoint control downward, while monitoring forward power out of the generator, and reflected power from the cavity. Relative forward power was monitored via the Micro-Now's internal power meter.

The data for reflected power versus generator relative forward power is shown below in Figure 27.

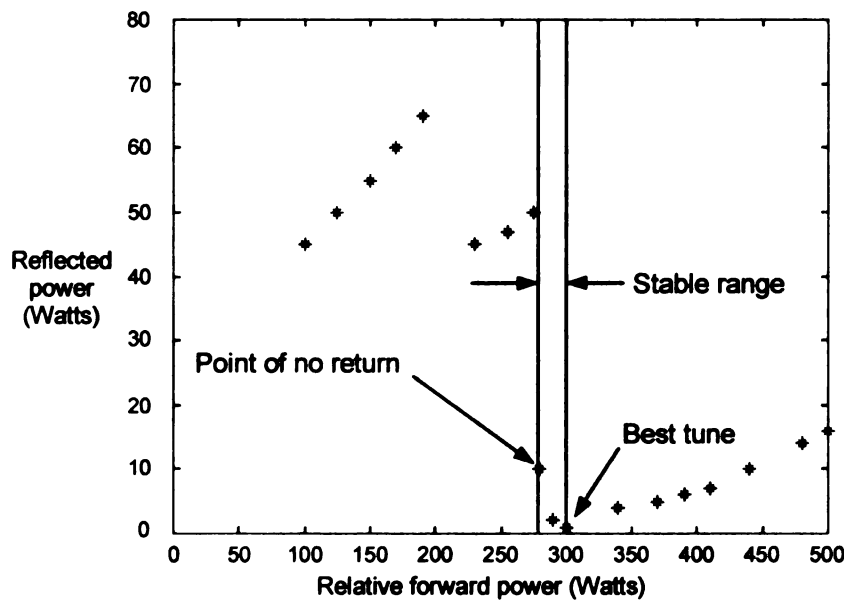


Figure 27: Standard system performance with generator power perturbation

The 'Point of no return' indicated above is the power setpoint lower limit before the system went unstable, and as mentioned above, occurred at about 10 Watts reflected.

The stable range indicated above is the forward power range below best tune for which the system remains stable.

The 'point of no return' could also have been found by perturbing the cavity height. This was attempted but the resolution of the servo system driving the short was limited to .1 cm minimum which made it difficult to determine the exact reflected power point at which the system went unstable.

It was found that increasing the setpoint power by any amount would not cause the system to go unstable. This is predicted in the model by observing (Figure 22) that plasma densities above the equilibrium point are always stable.

Perturbing the system by changing the cavity height resulted in the data shown below in Figure 28.

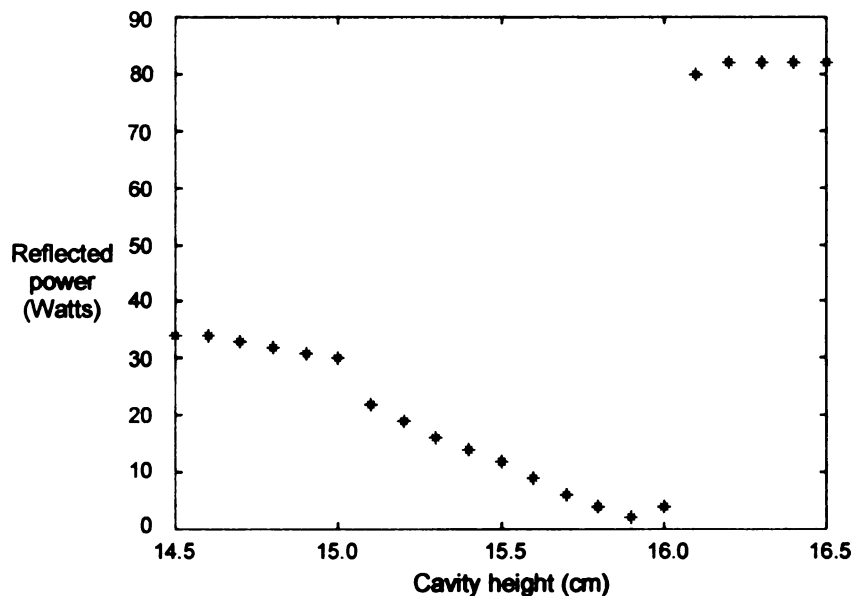


Figure 28: Standard system performance with cavity height perturbation

The rapid jump in reflected power occurred somewhere between 16.0 and 16.1cm as the height was increased. It should be noted that this data was taken with the cavity height moving in the increasing direction, (left to right in the plot). After the abrupt upward jump in reflected power, recovery was not accomplished until the cavity height

was brought all the way back to 13.7 cm. This hysteresis effect has been observed in several other studies of cavity type driven plasmas [11]-[19].

Standard System Analysis

The coefficient of cavity reactance/plasma resistance, 'a', was determined through the information found above. Since the most reflected power observed when the jump occurred was about 10 Watts, the lower limit of plasma density for stability was determined by linearly equating delivered power to plasma density. A power reflection coefficient of .05 represents 10 Watts reflected for 200 Watts forward. This 5% perturbation in delivered power (200-10) from the nominal operating point delivered power (200-0), represented about a 5% drop in plasma density.

Setting x' of Equation (1) above to zero and solving for the numerator polynomial using different values for the resonance/density coefficient 'a', it was determined that a value of $a = 8.0$ yielded solutions for plasma density at $4.34e17$ and $4.09e17$. These are the zeros of a plot similar to that of Figure 22 . These two solutions are different by a factor of about 6% which is close to that of the 5% plasma density ratio determined above to be the left side of the region of attraction of the standard system. The plot of the standard system differential equation with the 'a' coefficient set to 8 is shown below in Figure 29. As indicated below, the region of attraction is from the unstable equilibrium point, representing a plasma density of $4.09e17$, and up.

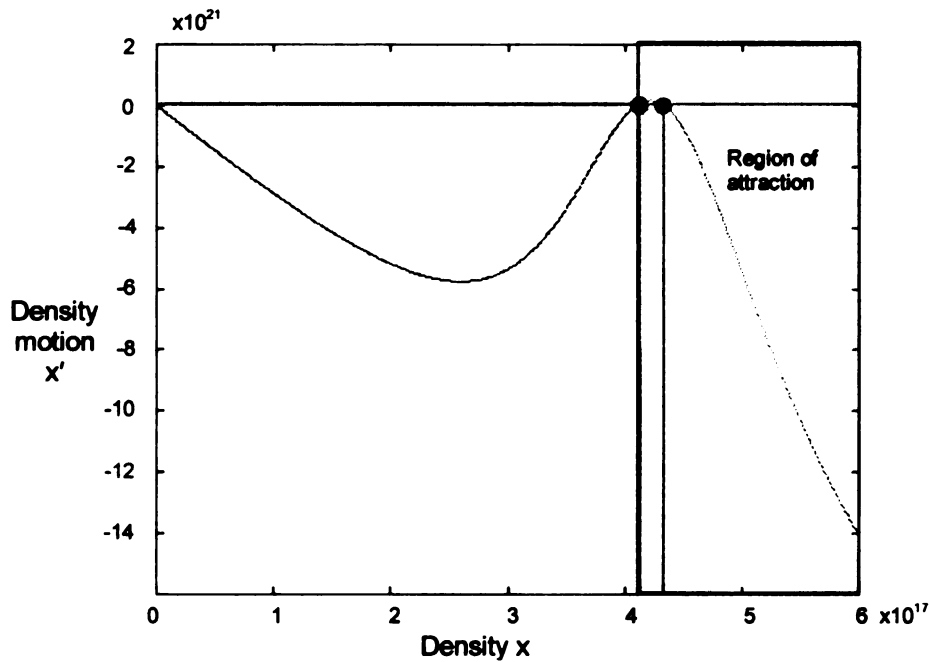


Figure 29: Standard system differential equation, resonance/density coeff 'a' = 8

Modified System

A large reactive offset was chosen to ensure a large effect and still remain within the power delivery capability of the microwave generator. Since the generator was capable of delivering 500 Watts into 50 ohms, a power reflection coefficient of .55 was chosen to ensure that at least 200 Watts could be delivered into the modified system with the reactive offset.

The system was modified as per Figure 18 above. The modified system schematic is shown below in Figure 30.

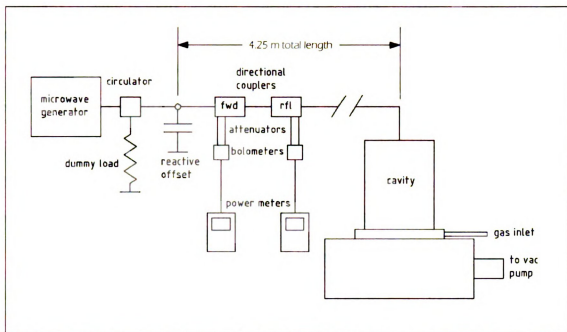


Figure 30: Modified system schematic

A photo of the reactive offset setup is shown below in Figure 31.

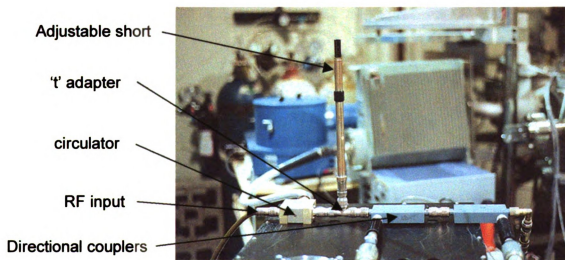


Figure 31: Modified system reactive offset

To create the offset, a General Radio 874-D20 adjustable shorted stub was connected in parallel to the transmission line with an 'N' type 't' adapter. To characterize the offset, one end of the 't' adapter was terminated with 50 ohms, and the impedance was observed

looking into the other end with an HP 8510 Network Analyzer. The impedance was measured to be about $16 - j55$ Ohms, representing a power reflection coefficient of .55. The model used for this stability analysis assumes that the reactive offset is a series element. Using a Smith chart, the effective series reactance with 50 ohms real was found by plotting a point along the 50 ohm circle that intersect a line segment of .55 power reflection coefficient away from the center. The resulting effective series impedance was $50 - j110$ Ohms. This transformation method is illustrated below in Figure 32.

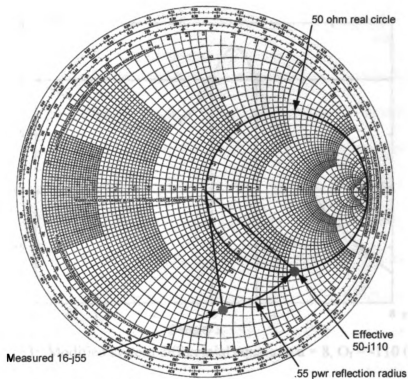


Figure 32: Determining effective reactive offset

The transmission line length between the power sensors and the cavity was chosen through repeated trial and error for best stability. To predict this length would have been too difficult given that the calculated length margin of error would have been an appreciable percentage of a wavelength at 2.45 GHz.

Model Verification

Figure 33 below is a plot of the modified system differential equation. The reactive offset was set to -110 Ohms, with the 'a' coefficient set to 8. The equilibrium points are now at about 3.75×10^{17} and 2.95×10^{17} . Equating plasma density to power, the second equilibrium point is about 20% below that of the first, representing a reflected power of 20% of indicated forward. Thus, for 200 Watts forward, the system should remain stable up to about 40 Watts reflected.

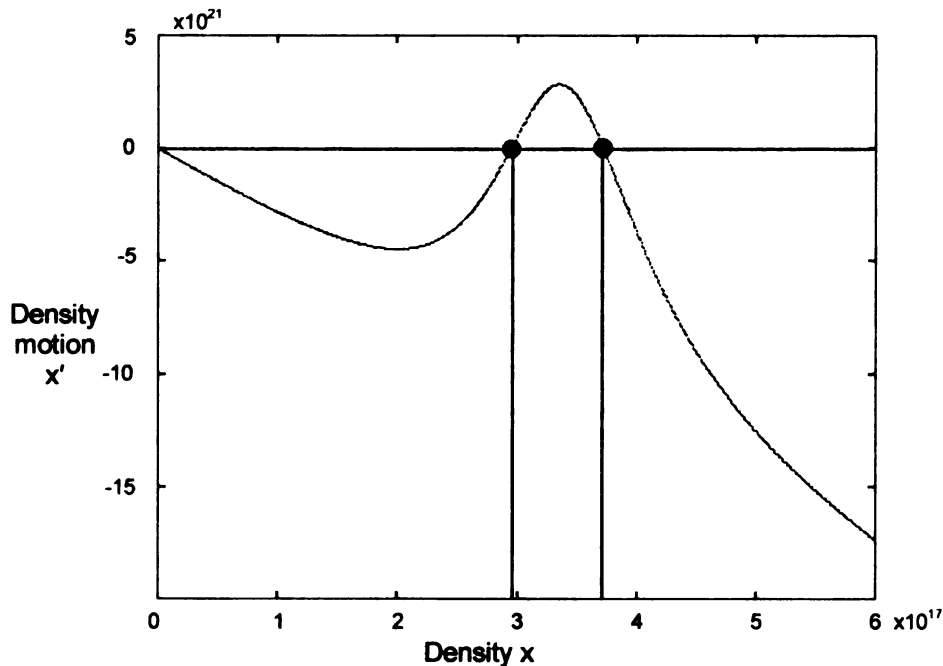


Figure 33: Modified system differential equation, $a = 8$, $O_f = -110$ Ohms

The power setpoint perturbation method was performed on the modified system via the sequence of steps outlined for the standard system, with the following results shown on the plot below, Figure 34:

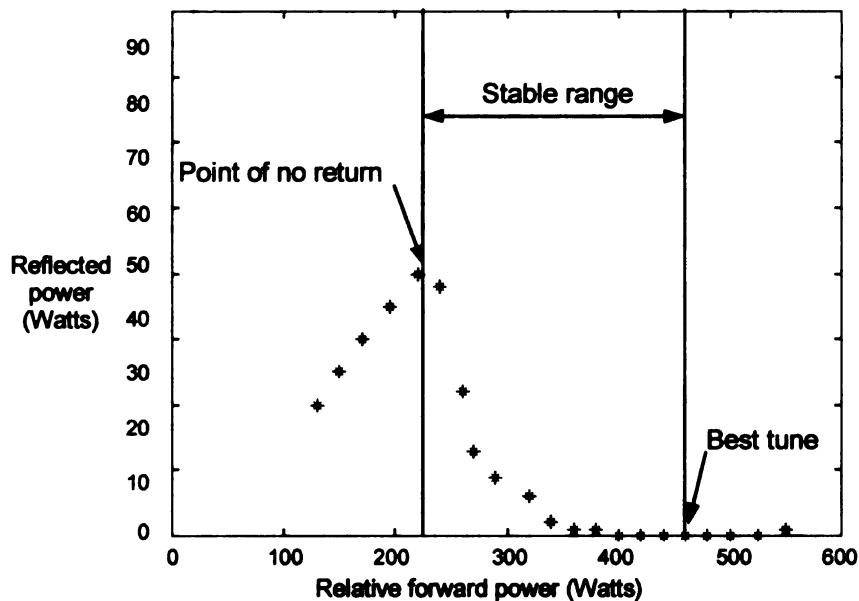


Figure 34: Modified system performance with generator power perturbation

Compare the modified system performance of Figure 34 above to the standard system performance of Figure 27. The maximum reflected power of 40 Watts is much larger than the standard system's 10 Watts reflected power. Also, the stable range is from 225 Watts to 480 Watts as compared to the standard system's 275 to 300 Watts.

Figure 35 below is a plot of the modified system's actual performance for cavity height perturbations. There was a rapid movement at about 30 - 50 Watts reflected where the plasma would still be lit but at a reduced density. More importantly, the high density plasma state would sometimes recover when the cavity height was returned from a high position, (up to 16.4), back down to the best tune position, (small amount hysteresis). In either direction of tuning, there was a small abrupt jump in reflected power around the 16.2 – 16.3cm position (30-50 Watts).

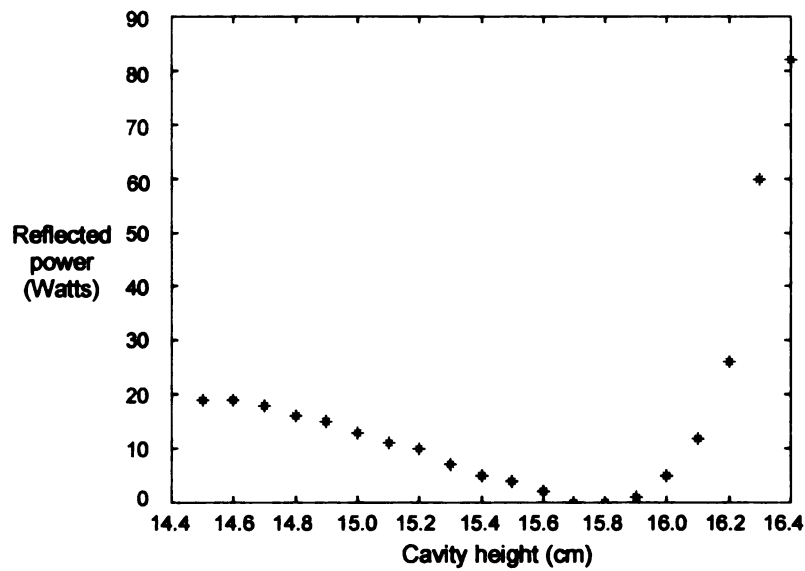


Figure 35: Modified system performance with cavity height perturbation

To show the cable length dependence upon the modified system's stability, the transmission line length was shortened by approximately $\frac{1}{4}$ wavelength. To model this condition, the conjugate of the offset is chosen, changing O_f from -110 to 110 Ohms. Figure 36 below is the modeled prediction of behavior, indicating no stable equilibrium points, (dn/dt always less than 0), other than at zero density.

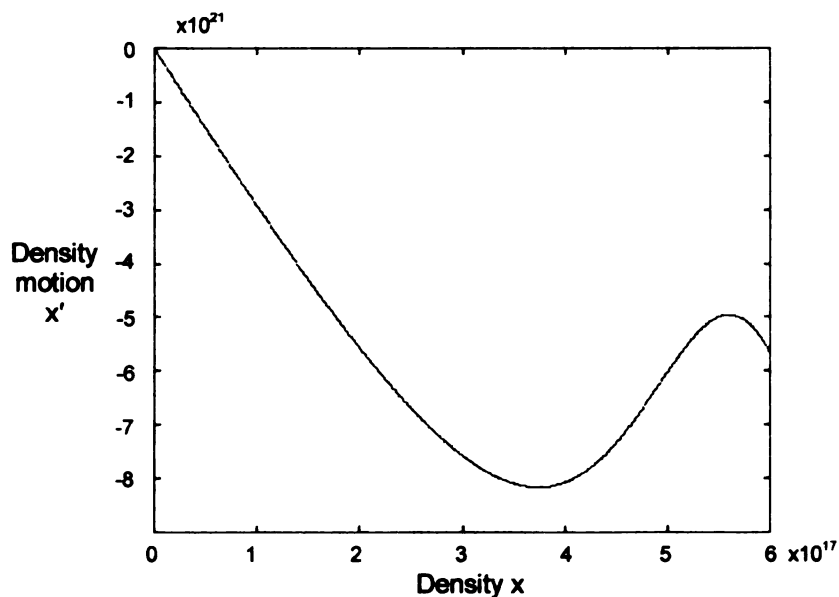


Figure 36: Modified system differential equation with $\frac{1}{4} \lambda$ shorter transmission line

Figure 37 below is a plot of the modified system's actual performance with the shorter transmission line length. There was no stable operating point at zero reflected power and the recovery position for the cavity height was well below 14cm.

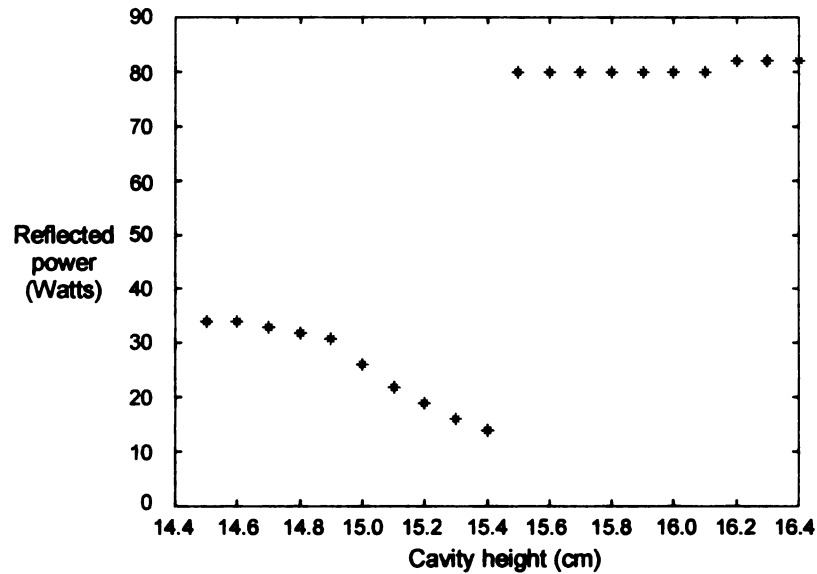


Figure 37: Modified system performance with $1/4 \lambda$ shorter transmission line

Conclusions

The phenomenon of plasma system stability as a function of system parameters outside of the plasma itself is clearly shown in the preceding analysis. This analysis treated the plasma as if it were a simple device with a conductivity linearly proportional to power, and with a first order arbitrary time response. The microwave cavity was treated as a lossless, single-mode resonant device, with its reactive component having a linearly proportional dependence on plasma density. All other losses external to the plasma were neglected. There were no nonlinearities or discontinuities assumed in any of the component models. With all of these seemingly gross approximations, stability prediction was still reasonably well achieved. With a single first order differential equation it was predicted that system stability could be increased or decreased through the manipulation of the transmission line length and the microwave power supply's effective source impedance. Implementation of such a modified system confirmed these predictions using two different types of perturbation.

It is concluded from these results that the modeling of a plasma system from a 'controls' point of view is a valid approach and that many observed plasma system instabilities may be attributed to this systematic phenomenon. This does not preclude any direct nonlinearities or hysteresis effects of the plasma and its interactions with its physical surroundings. Discontinuities of RF/microwave driven plasma sources are quite common, especially in environments of complex shapes, and/or changing process chemistries. However, it may behoove the system designer to be aware of this more fundamental system-based source of potential instability before attempting to deal with more complex behaviors encountered in plasma processing.

The models used for this analysis have pointed out one major contributor to system instability through the cavity resonance to plasma density coefficient, 'a'. If plasma launching devices could be designed to reduce the effect that changing plasma density has upon resonance, these potential instabilities could be minimized.

The system models could obviously be greatly improved, enabling even more predictive accuracy. For example, given a more accurate relationship between the cavity height and input impedance to the cavity, the height versus reflected power plots for the actual and calculated data could have been directly compared. The two major areas for improvement are in the models for the plasma and for the cavity/plasma interactions.

The following are some suggestions for model enhancements:

Plasma Model potential improvements:

1. Include the major nonlinearity of plasma ignition hysteresis. A minimum excitation energy is required to ignite a plasma. The plasma will not extinguish until an excitation energy is reached that is lower than the ignition energy.
2. Better characterize density as a function of absorbed power.
3. Characterize the ignition and density/power functions for different gases.

Cavity Model potential improvements:

1. Characterize cavity input impedance as a function of cavity/probe heights and plasma density through numerical analysis [20].
2. Include functions for other resonant cavity modes, and the relationships that determine which modes dominate for which conditions.
3. Include cavity wall losses as functions of calculated tangential magnetic fields.

Other model items that could provide overall system model enhancement:

1. Transmission line losses as a function of power and mismatch.
2. Realistic circulator model with losses and nonlinear behavior.

These model improvements are certainly realizable and would go a long ways towards building a 'virtual' plasma system that could be the foundation of a more in-depth model used to predict much more complex behaviors of RF/microwave driven semiconductor plasma processes and machines.

REFERENCES

- [1] A. J. Hatch, L. E. Heuckroth, "Retuning Effects and Dynamic Instability of a Radio-Frequency Capacitive Discharge," *Journal of Applied Physics*, vol. 41, #1, pp 1701-1706, March 1970
- [2] P. W. Lee, S. W. Lee, H. Y. Chang, "Undriven Periodic Plasma Oscillation in Electron Cyclotron Resonance Ar Plasma," *Appl. Phys. Lett.*, vol 69, #14, pp 2024-2026, Sept 1996
- [3] J. Assmusen, R. Mallavarpu, J. R. Hamann, H. C. Park, "The Design of a Microwave Plasma Cavity," *Proceedings of the IEEE*, pp. 109-117, 1974
- [4] M. A. Lieberman, A. J. Lichtenberg, *Principals of Plasma Discharges and Materials Processing*. New York: Wiley, 1994, pp. 304-308
- [5] Based on conversations and data from Mark Perrin, Ph.D. candidate, Michigan State University, Feb 2000
- [6] M. A. Lieberman, A. J. Lichtenberg, *Principals of Plasma Discharges and Materials Processing*. New York: Wiley, 1994, pp. 164-166
- [7] M. A. Lieberman, A. J. Lichtenberg, *Principals of Plasma Discharges and Materials Processing*. New York: Wiley, 1994, pp. 390-392
- [8] R. A. Chipman, *Theory and Problems of Transmission Lines*, New York, McGraw-Hill, 1968
- [9] H. K. Kahlil, *Nonlinear Systems, 2nd Edition*, New Jersey, Prentice Hall, 1996
- [10] P.U. Mak, "An Experimental Evaluation of a 12.5 cm Diameter Multipolar Microwave Electron Cyclotron Resonance Plasma source," Ph.D. dissertation, Michigan State University, 1997
- [11] P. L. Colestock, "Radio-Frequency Coupling to Plasmas," *J. Vac. Sci. Technol. A*, vol. 6, pp 1975-1983, 1988
- [12] P. Leprince, G. Matthieussent, "Resonantly Sustained Discharges by DC Current and High-Frequency Power," *Journal of Applied Physics*, vol. 42, #1, pp 412-416, Jan 1971
- [13] I. Ghanashev, M Nagatsu, G. Xu, H. Sugai, "Mode Jumps and Hysteresis in Surface-Wave Sustained Microwave Discharges," *Jpn. J. Appl. Phys.*, vol. 36 (1997), pp 4704-4710, Part1, #7B, July 1997

- [14] E. S. Aydil, J. A. Gregus, R. A. Gottscho, "Multiple Steady States in Electron Cyclotron Resonance Plasma Reactors," *J. Vac. Sci. Technol. A* vol. 11 #6, pp 2882-2892, 1993
- [15] M. A. Jarnyk, J. A. Gregus, E. S. Aydil, R. A. Gottscho, "Control of an Unstable Electron Cyclotron Resonance Plasma," *Appl. Phys. Lett.* Vol. 61, #17, pp 2039-2041, April 1993
- [16] Y. Matsunaga, T. Katp, "Simple Model Analysis of Hysteresis Phenomenon of Gas Discharge Plasma," *Journal of the Physical Society of Japan*, vol. 66, #1, pp. 115-119, Jan 1997
- [17] H. Sun, L. Ma, L. Wang, "Multistability as an Indication of Chaos in a Discharge Plasma," *Physical Review E*, vol. 51, #4, pp. 3475-3479, April 1995
- [18] R. J. Zhan, X. C. Jiang, "Jumps and Hysteresis Effects in CH₄-H₂ Plasma Discharges," *J. Phys. III France* 5, pp. 197-202, 1995
- [19] O. Popov, J. Assmusen, *High Density Plasma Sources*. New Jersey: Noyes Publications, 1995, pp. 275-276
- [20] L. C. Kempel, P. Rummel, T. Grotjohn, and J. Amrhein, "*Finite Element Method for Designing Plasma Reactors*," 16th Review of Progress in Applied Computational Electromagnetics, Monterey, CA, March 2000.

MICHIGAN STATE LIBRARIES



3 1293 02318 6392